ISSN: 2447-3359

REVISTA DE GEOCIÊNCIAS DO NORDESTE

Northeast Geosciences Journal

v. 9, nº 2 (2023)

https://doi.org/10.21680/2447-3359.2023v9n2ID32105

Physical simulation of overland flow with pedosediment concentration between 6 and 8%

Simulação física de escoamentos superficiais com concentração de pedosedimentos entre 6 e 8%

Julio Cesar Paisani[1]; Antonio Carlos de Barros Côrrea[2]; Rafael Manica[3]; Flávia Jorge de Lima[4]; Gustavo Gallardo Aere[5]; Matheus Vinícius dos Santos[6]; Josielle Samara Pereira[7]

[1] State University of Western Paraná, PaleoEnvironmental Studies Center (NEPA), Francisco Beltrão/PR, Brazil. Email: juliopaisani@hotmail.com; julio.paisani@unioeste.br
ORCID: https://orcid.org/0000-0002-8911-6477

[2] Federal University of Pernambuco, Department of Geographical Sciences (DCG), Recife/PE, Brazil. Email: dbiase2001@terra.com.br
ORCID: https://orcid.org/0000-0001-9578-7501

[3] Federal University of Rio Grande do Sul, Institute Hydraulic Research (IPH), Porto Alegre/RS, Brazil. Email: manica@iph.ufrgs.br
ORCID: https://orcid.org/0000-0002-0527-1374

[4] Federal University of Alagoas, Sertão Campus, Delmiro Gouveia/AL, Brazil. Email: flavia.lima@delmiro.ufal.br
ORCID: https://orcid.org/0000-0003-4176-5854

[5] State University of Western Paraná, PaleoEnvironmental Studies Center (NEPA), Francisco Beltrão/PR, Brazil. Email: gustavogallardoaere@outlook.com
ORCID: https://orcid.org/0009-0007-4924-3256

[6] State University of Western Paraná, PaleoEnvironmental Studies Center (NEPA), Francisco Beltrão/PR, Brazil. Email: matheusvini.geo@gmail.com
ORCID: https://orcid.org/0000-0003-3031-7925

[7] State University of Western Paraná, PaleoEnvironmental Studies Center (NEPA), Francisco Beltrão/PR, Brazil. Email: josy.samara@hotmail.com
ORCID: https://orcid.org/0000-0002-4309-1833

Abstract: Based on the results of previous physical experiments in the laboratory, the aim of this study was to verify whether overland flow simulations with sediment concentrations of 6 to 8% generate deposits similar to flows with lower (~ 3%) or higher (>14%) relative concentrations. Two flow replications exhibited concentrations in these ranges and their mean velocities, Froude and Reynolds numbers, and their deposits were analyzed. A supercritical-turbulent flow regime prevailed between the initial conditions and arrival on the sedimentation plane, which gradually changed to subcritical-laminar flow until waning. Surface structures of the deposits are similar in layout, but differ in width, preservation of vertical accretion, and groove mark development, as well as in relation to bed microstratigraphy, which is mainly due to the thickness, organization, and number of laminations. The fact that the deposits are formed by more than one lamination shows the effects of the tail/body of the flow in re-settling the materials previously deposited by the head of the flow. Surface structures and bed microstratigraphy coincide with those found in both lower and higher relative concentration flow deposits, meaning that the sediment concentrations of the analyzed flows express a continuum between low density flows and transitional flows between low and high densities.

Keywords: Overland flow; Pedosediments; Microstratigraphy.

Resumo: Com base em resultados prévios de experimentação física em laboratório o objetivo desse trabalho foi verificar se simulações do escoamento superficial com concentrações de pedosedimentos de 6 a 8 % geram depósitos semelhantes a fluxos de menor (~ 3 %) ou de maior (>14 %) concentração relativa. Duas repetições de fluxos exibiram concentrações nesses intervalos e foram analisadas suas velocidades médias, números de Froude e Reynolds, e seus depósitos. Predominou regime de fluxo supercrítico-turbulento entre as condições iniciais e sua chegada no plano de sedimentação, passando paulatinamente a subcrítico-laminar até minguar. Estruturas de superfície dos depósitos são semelhantes quanto à disposição, mas diferiram quanto a largura, preservação da acreção vertical e desenvolvimento de marcas de sulcos; bem como em relação a microestratigrafia de leito, sobretudo pela espessura, organização e o número de laminações. O fato de os depósitos serem formados por mais de uma laminação mostra os efeitos da cauda/corpo do fluxo em resedimentar os materiais previamente depositados pela cabeça do fluxo. Estruturas de superfície e microestratigrafia de leito coincidem com aquelas encontradas tanto em depósitos de fluxos de menor e de maior concentração relativa, acarretando que as concentrações de sedimentos dos fluxos analisados expressam o contínuo entre fluxos de baixa densidade e fluxos transicionais entre baixa e alta densidades.

Palavras-chave: Escoamento superficial; Pedosedimentos; Microestratigrafia**.**

Received: 04/08/2023; Accepted: 14/09/2023; Published: 05/10/2023.

1. Introduction

Overland flow, also known as wash, sheet flow, sheet wash, runoff, surface runoff and water flow, is a crucial geomorphic process in the morphodynamics of landscapes, especially in the Brazilian semi-arid region, where the rainfall regime associated with low-density vegetation cover contributes to the development of diffuse unchanneled runoff (FONSECA et al., 2017). With the advancement of land use for food production and progressive soil loss due to inadequate management, landscape responses to overland flow have received attention in recent decades, especially in attempts to mitigate the effects of tillage erosion. However, little is still known about the processes and products of overland flow sedimentation, which leads some geoscientists to classify its deposits as "slope alluvium" (MILLER; JULLIERET, 2020). This interpretation assumes that overland flow generates flows with dynamic behavior similar to the behavior of channeled water (e.g., river dynamics), whose properties follow the Newtonian rheological model in which the flow has a low sediment concentration and suffers the direct interference of gravity, which in turn interferes with sedimentation (BENVENUTI; MARTINI, 2002).

Sandy stratigraphic records on hillslopes and their surroundings are interpreted as resulting from overland flow in Quaternary sequences of temperate to subtropical areas with different rainfall regimes (BERTRAND et al., 1995; BLIKRA; NEMEC, 1998; NEMEC; KAZANCI, 1999; OLIVEIRA et al., 2001; 2008; VENTRA et al., 2013). In northeast Brazil, under the transitional semi-arid to sub-humid climatic environment of the Baixa Verde Massif, in the state of Pernambuco, sub-contemporary deposits mantling pedimented slopes present clearcut characteristics of lower Holocene upslope gravitational colluvium flows reworked by laminar erosion (CORREA; MONTEIRO, 2020). Due to their historical chronology and partial preservation of parallel laminated structures, these materials were interpreted as resulting from overland flow under vegetation cover suppression and bare soil exposure following the occupation of the area in post-colonial times.

Exclusively attributing the Newtonian rheological model to the overland flow sedimentation process assumes that this flow type always behaves as a low-density flow. In reality, the sediment concentration changes the dynamic behavior of the flow and implies that gravity also acts directly on the sediment, promoting a different dynamic and different rheological behavior to the Newtonian model, resulting in non-Newtonian flows or, simply, high-density flows. Furthermore, there are situations where the dynamic behavior is transitional between low and high-density flows (DASGUPTA, 2003). The literature lacks consensus regarding the sediment concentration values determining a flow's classification as low, transitional, or high density (SHANMUGAM, 1996). Absolute values for the limit between low and high-density flows are difficult to establish because they depend on grain size distribution, clay content, and rheological variables (PIERSON; COSTA, 1987; SHANMUGAM, 1996; MANICA, 2012). In this study, we sought to artificially reproduce different flow concentrations with properties similar to overland flow, considering that laboratory experimentation is a helpful tool for understanding sedimentation processes and products under controlled conditions (BENNET et al., 2015). Thus, the experiment aimed to understand the relationship between sediment concentration and the resulting sedimentary fabrics/structures. To date, fluids with a solid fraction of pedosediments (soil aggregates and other granular pedological constituents – Paisani et al., 2023a, c 2023b) have been generated at low (Cv ~ 3%) and transitional to high volumetric concentrations (Cv 14-25%), which means there are flows in low, transitional, and high-density categories for fluids made up of pedosediments. However, doubt remains as to whether flows with intermediate concentrations (between 3 and 14%) generate deposits similar to low or transitional to high-density flows, which is precisely the question that this study aims to answer.

2. Methods

The experimental station at the Center for PaleoEnvironmental Studies Laboratory at Unioeste (NEPA) was used to generate flows with different pedosediment concentrations, simulating a straight hillslope segment followed by a slope break to create a space for sediment accumulation. The slope break resembles a change in morphology, such as the passage from the base of a hillslope to the bottom of a catchment (hollow), valley bottoms of hierarchical order lower than the fourth order in Strahler's classification (STRAHLER, 1952), or pediment ramps. The experiment is composed of three independent parts: a) water storage/release cylinder; b) flow displacement ramp (unchanneled flume) simulating a straight hillslope segment; and c) deposition plane simulating an area of sediment accumulation (Figure 1).

The ramp was adjusted to an inclination of 23º, while the sedimentation plane had an inclination adjusted to 4º. Measuring rulers were installed on both (accuracy of 1 mm and spaced at 12 cm), fixed to a frame perpendicular to the flow direction to determine the respective depths based on Ali et al. (2011) (Figure 1). The experimental method applied in this study does not propose a scale model with direct dynamic similarity to natural deposits. Instead, it proposes an empirically controlled approach to the most common field contexts for the occurrence of overland flow (PAOLA et al., 2009). The affinity with the field context is mainly due to (a) the pedosediments previously detached from the soil and available for transport by overland flow over the slopes, a dominant constituent element in overland flow (ALBERTS et al., 1980; LIU et al., 2020); (b) the size and composition of pedosediments; (c) unconfined flows that mix water and sediments on the hillslope; and (d) the topography marked by a break in gradient between the transport sector (hillslope) and the sedimentation sector (accommodation space).

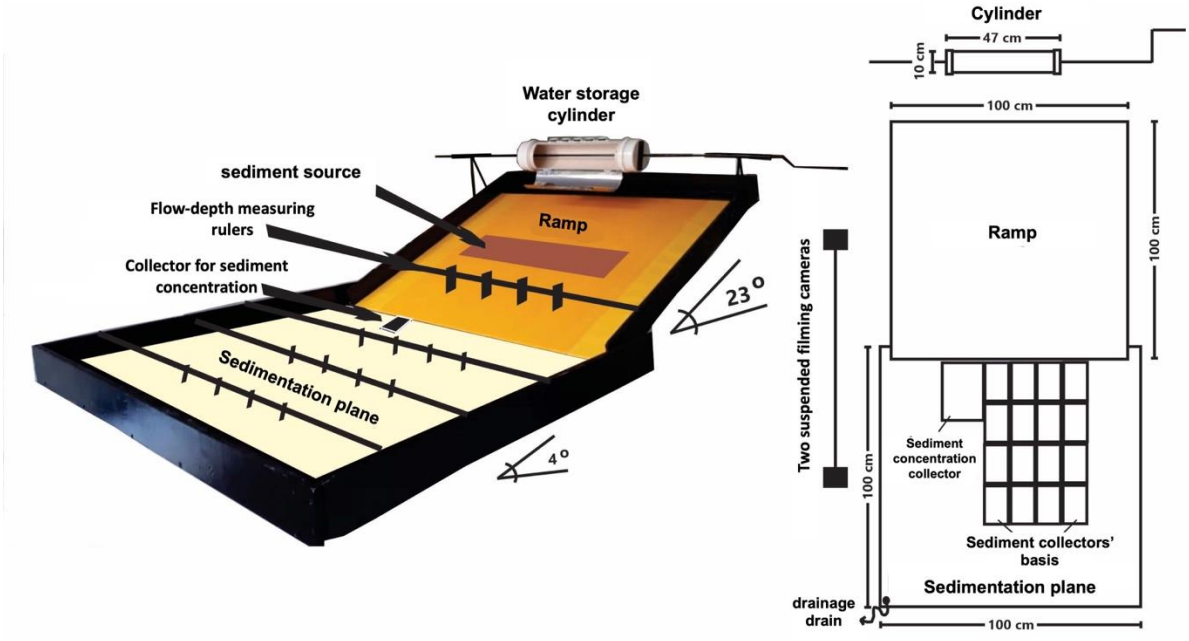

Figure 1 – Experimental station at the Center for PaleoEnvironmental Studies Laboratory at Unioeste (NEPA).
Source: Authors (2023).

The solid fraction of the flows used in the experiment consisted of natural pedosediments originating from Bi and BC horizons of Cambisols and litholic Neosols exposed to the surface, deposited at the foot of the hillslope as a colluvium of soil aggregates. According to the Wentworth scale (WENTWORTH, 1922), the pedosediments were separated in particle size fractions by sieving and ranged from very fine sand to fine pebbles. These sediments were placed in the center of the ramp in proportions of 0.167 to 212 kg of dry mass (Figure 1). The admixture of water and sediment was obtained spontaneously by releasing the water from the cylinder in volumes ranging from 250 to 300 ml. The volumetric concentration (Cv %) of sediments/solids in the fluids was determined from rectangular collectors (0.16 x 0.13 x 0.13 m) installed at the head of the sedimentation plane (Figure 1), considering 998 and 2,180 kg.m-3 as the average density of water and sediments, respectively. Finally, fourteen repetitions were carried out, of which only two (R13 and R14) reached the desired concentrations (Cv 3% > intermediate < 14%), while the others had Cv > 14%.

The average speed of each flow was measured by filming both the ramp and the sedimentation plane by extracting the flow displacement per unit of time (Vm $m.s^{-1}$). Given the changes in the Vm of each flow, as it moved through the sedimentation plane, the Vm was divided into three stages: arrival, intermediate, and waning. The average parameters of Froude (Fr) and Reynolds (Re) numbers were then determined as follows:

Formula 1 - Froude number (Fr)

$$Fr = V_m/\sqrt{(g.h)}$$

in which, Fr is the Froude number, V_m is average flow velocity, g is gravity, and h is the average flow depth.

Formula 2 - Reynolds number (Re)

$$Re = V_m.h/\nu$$

in which, Re is the Reynolds number, V_m is average flow velocity, h is average flow depth, and v is the kinematic viscosity of the water.

The analyzed hydraulic parameters were compared with parameters similar to those obtained for flows of low (~ 3%) and transitional to high (> 14%) relative volumetric concentration (PAISANI et al., 2023a, c v.24, n.3, 2023c). The sediments of the two replications (R13 and R14) that reached the desired intermediate concentrations were collected and impregnated (mixture of epoxy resin, acetone, and amine-based drying agent) in a vacuum (15 mm Hg), dried (in a 32º oven and open-air) until curing, and laminated parallel and transverse to the flow direction. The blocks were processed at NEPA Lamination LabMulti, where re-impregnation (obliteration of imperfections) was carried out, before mounting on glass to produce thin sections of each flow direction with dimensions of 7.2 x 2.5 cm up to a thickness of approximately 30 µm. The sections were analyzed in the NEPA Optical Microscopy LabMulti with a Leica DM 2500 P petrographic microscope with a 1.25x objective, and image capture was carried out using a Leica EC 3 camera and the Leica Application Suite (LAS EZ) software, version 1.4. From this procedure, laminations were distinguished, and the following attributes were recognized: average thickness (mm), upper limit, texture, composition, roundness-sphericity, selection, and fabric. The diagrams of Campbell (1967), Powers (1953), and Harrel (1983) were used to determine the upper limit, roundness-sphericity, and selection, respectively. The grain size percentages were based on the Fitzpatrick diagram (1980) and the textural class on the conglomerate diagram (NICHOLS, 1999).

3. Results and discussion

3.1 Parameters and hydraulic indices

Given the spontaneous mixing conditions of water and sediments, the Cv of flows R14 and R13 ranged from 6.19 to 8.76%, respectively, within the flow limits of greater than 3% and less than 14%, as already mentioned. The Vm of flows with Cv ~3% and Cv > 14% measured in the initial conditions (ramp) varied from 1.71 to 14.66 $m.s^{-1}$, with flows with Cv ~3% having relatively higher Vm than flows with Cv > 14% (Figure 2). Flows R13 and R14 had intermediate velocities of 0.66 to 1.08 $m.s^{-1}$, respectively. It can be seen that Vm has an inverse correlation with sediment concentration, decreasing proportionally with increases in concentration, which in turn entails an increase in flow viscosity (Figure 2), as expected. The Vm of the flows decreased significantly from the ramp to the sedimentation plane, especially for flows with concentrations lower than 6.19% (R14), and gradually decreased for other flows with higher concentrations (Figure 2). The high Vm of the flows in the initial conditions is higher than that obtained in experiments with a lower flume slope than in the present study, both in laboratory and field conditions (ABRAHAMS et al., 1986; ALI et al., 2011; GUO et al., 2017; LIU et al., 2020), which happens due to the high slope of the ramp (23º). In turn, the high initial Vm of the flows resulted in significant values of Froude and Reynolds numbers (Figure 2).

The Froude number, which relates the average flow velocity to the force of gravity and its average depth, was mainly above 1 for the initial conditions (ramp), indicating supercritical behavior (fast flow). Flows with lower sediment concentrations ≤ 8.76% (R13) had higher values, between 6 and 10, while the Froude number values were lower for flows with relatively higher concentrations (Figure 2). The Froude number of the flows along the sedimentation plane is relatively lower than under initial conditions, becoming less than 1 as the flows lose acceleration on the sedimentation plane. In this case, the flow becomes subcritical, passing through a hydraulic jump between the different flow stages on the sedimentation plane. The sudden increase in the Froude number was detected in the intermediate flow stage for some flows with Cv > 14 % (Figure 2). This is supposedly due to the increased flow depth with the flow's tail-and-body thrust wave over its head. This situation could result from breaking roll waves, as postulated by mathematical models of unidirectional flows (CARTIGNY et al., 2014). However, for the physical conditions of the experiment reported here, it can be said that

there was an increase in the flow depth and a respective increase in the Froude number due to the thrust wave (PAISANI et al., 2023a, c), as observed by the sequence of images captured from R13 (Figure 4). In general, a supercritical flow regime (Fr > 1) predominated between the initial conditions and its arrival on the sedimentation plane, gradually becoming subcritical (Fr < 1) until it subsided, with displacement on the sedimentation plane marked by a hydraulic jump.

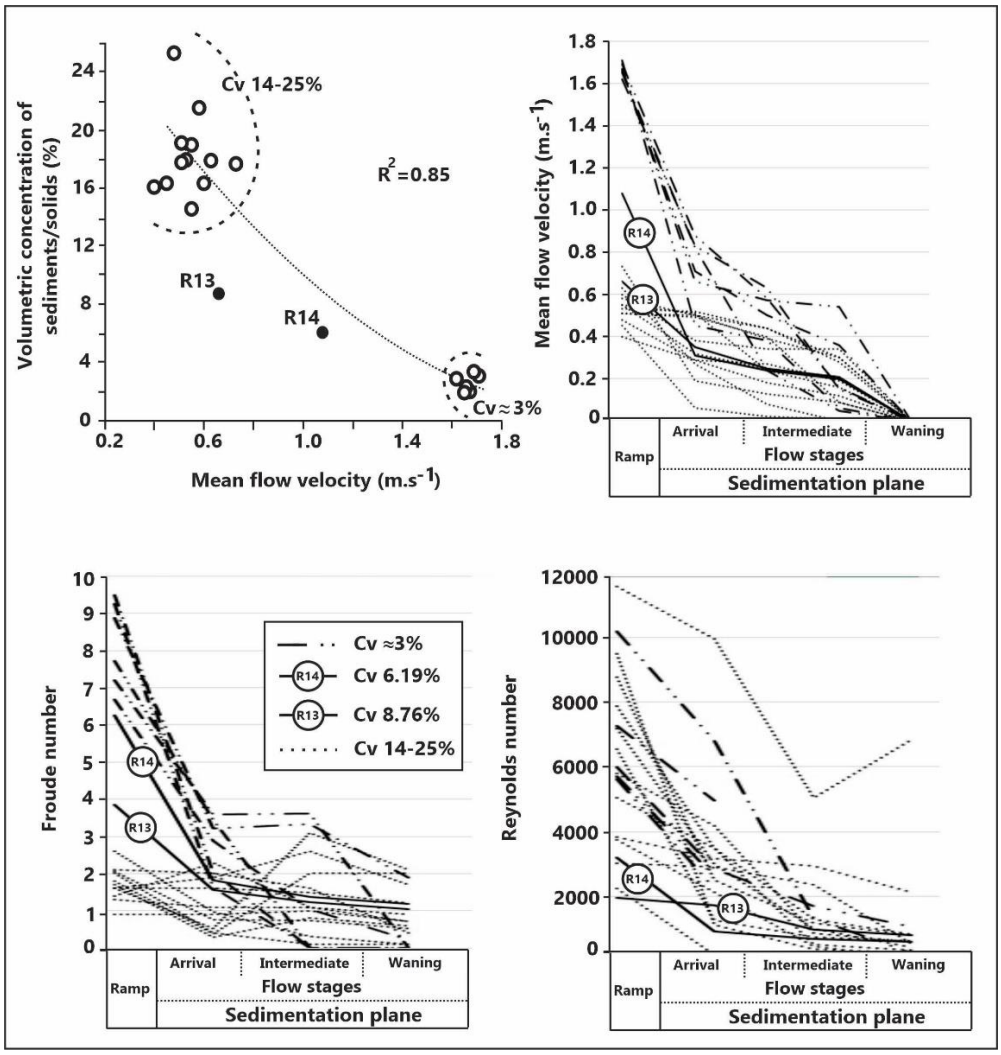

Figure 2 – Parameters and hydraulic indices extracted from flows with different pedosediment volumetric concentrations obtained at experimental station of overland flow simulation
Source: Authors (2023).

The Reynolds number varied from 11,568 to 2,243 for the initial conditions (ramp), becoming lower in the different flow stages of the sedimentation plane until reaching a minimum of 30 in the waning flow stage (Figure 2). For the initial conditions and the arrival of flows on the sedimentation plane, Reynolds numbers greater than 2,000 predominated, while from the intermediate flow stage, the resulting values were between 4,000 and 52 (Figure 2), with no correlation between the Reynolds number and the initial Cv. Finally, a Reynolds number (Re) > 2,000 indicates turbulent flow, while the interval 500 < Re < 2,000 characterizes a transition zone in which the flow is sometimes laminar and sometimes turbulent, whereas a Re < 500 indicates laminar flow.

3.2 Surface structure and bed microstratigraphy

Sediment deposits resulting from flows generated at the experimental station enabled analysis of the surface structure and bed microstratigraphy. Thus, those resulting from flows R13 (Cv 8.76) and R14 (Cv 6.19%) were analyzed using images of filming and thin sections, respectively.

Flows R13 and R14 generated deposits with similar surface structures in the elongated arrangement, marginal dikes, vertical accretion, and scour marks, although they differed in deposit width, preservation of vertical accretion, and rill mark development (Figure 3). The vertical accretion, the elongated arrangement, and the marginal dykes are surface structures found in flows of Cv >14%. In comparison, scour and rill marks are surface structures found in experimental flows of Cv ~3% (PAISANI et al., 2023a, c v.24, n.3, 2023c). When analyzing the footage of the flows responsible for the deposits of fluids R13 and R14, it was observed that the scour and rill marks were generated by the thrusting of the flow's tail and body over its head (Figure 4). This process supposedly occurs due to the more significant relative deceleration of the head due to its higher sediment content (PAISANI et al., 2023a, c). This overthrust did not promote a significant increase in flow depth, as it did not alter the decreasing trend in the Froude number (Figure 2), as suggested for some flows with Cv > 14%.

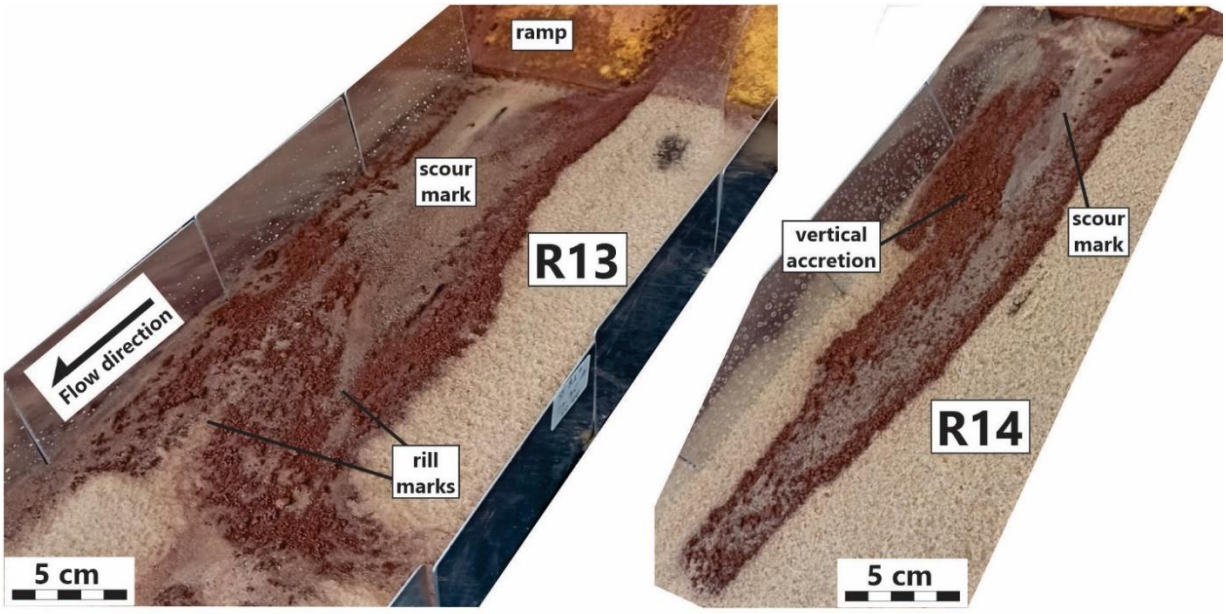

Figure 3 – Surface structure of flow deposits R13 (Cv 8.76 %) and R14 (Cv 6.19 %).
Source: Authors (2023).

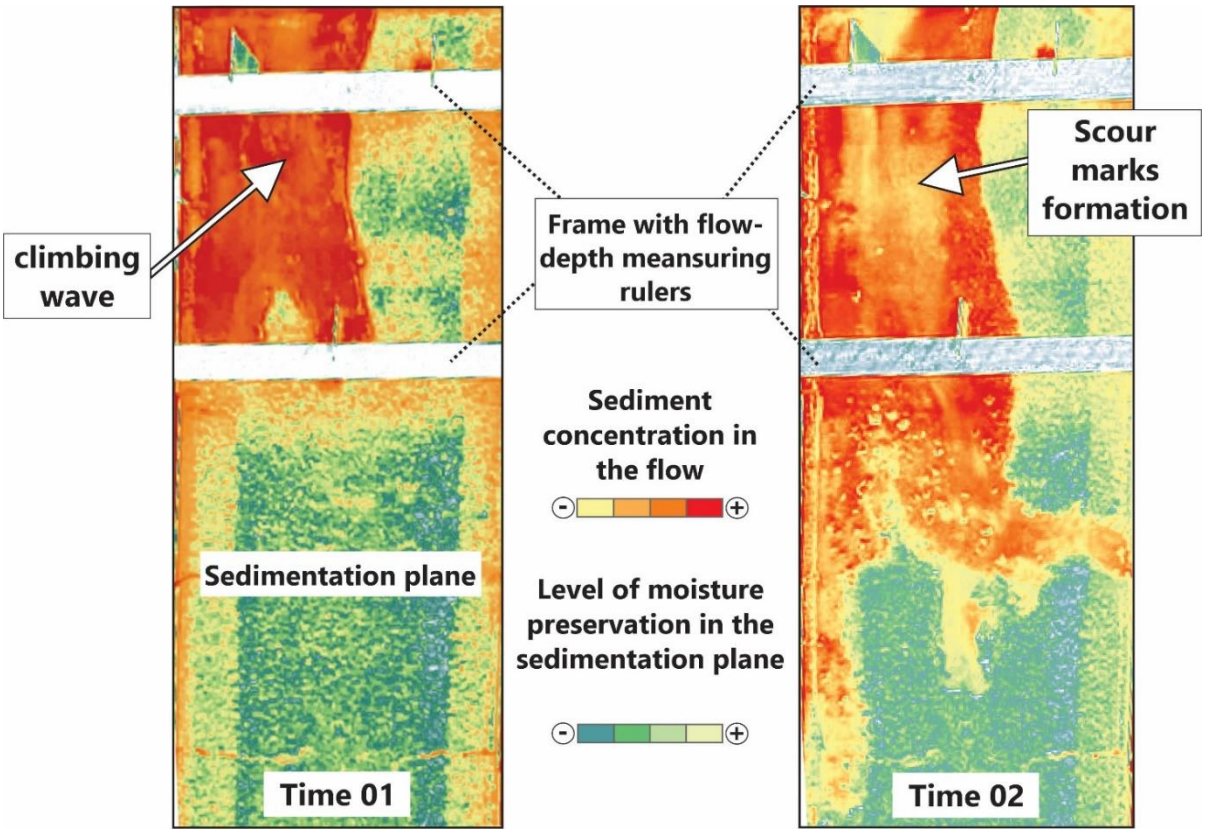

Figure 4 – Sequence of images captured by filming flow R13 (Cv 8.76 %). The digital analysis permits the observation of initial scour marks following the climbing of the flow's tail and body over the flow's head.
Source: Authors (2023).

The R13 and R14 deposits are distinct, mainly due to their thickness, organization, and number of laminations (Figure 5, Table 1). Deposit R13 (Cv 8.76%) has thin laminations (1.58 to 1.63 mm thick), with predominantly continuous-wavy-non-parallel surface boundaries, sandy texture, maximum grain size corresponding to very coarse sand, with a composition of pedosediment mixed with arkose quartz from the sedimentation plane, poor selection, and massive to inverse fabric with escaping interstitial fluids (air or water). On the other hand, the R14 deposit (Cv 6.19%) displays an erosional depression with asymmetrical concave morphology, in which the laminations are thicker than in R13, becoming laterally thinner. The surface limit of the laminations is predominantly continuous-wavy-non-parallel, with a texture varying from sand to fine gravel with a composition of pedosediment mixed with arkose quartz from the sedimentation plane. Selection is poor to moderate, and the fabric varies from massive to inverse or inclined, with escaping interstitial fluids (air or water). Cut and fill structures are observed where the erosional depression occurs.

Thin sections transverse to deposits R13 and R14 revealed a sequence of ridges and cavities, with the occurrence of surface structures like thinning marks in R14 (Figure 5). The longitudinal thin sections of the scour marks of the R13 deposit exhibit sediments that do not enable the laminations to be distinguished due to the homogeneity in the mixture of pedosediments with the arkose quartz from the sedimentation plane, with only two being identified, with similar internal and external organizations (Figure 5, Table 1). In the R14 deposit, it was possible to distinguish laminations, mainly due to the predominance of a sandy texture and the exclusively massive fabric.

Some morphological aspects stand out from the analysis of the longitudinal and transversal thin sections of the deposits and the longitudinal sections established in the sector with scour marks. The fact that the deposits are formed by more than one lamination shows the effects of the tail and body of the flow in resedimenting the materials previously deposited by the head of the flow. This behavior is similar to that observed in flows with higher relative volumetric concentration that suffered a gradual deceleration (Cv 14-25%). However, in the present context, it expresses the more significant dilution of

the tail and body of the flows. Galaxy-like microstructures typical of flows with higher relative volumetric concentration (Cv 14-25%) were not identified. The discontinuous or continuous, wavy, and non-parallel external organization is typical to both low (Cv ~ 3%) and transitional to high (Cv > 14%) relative volumetric concentration deposits of pedosediments. It can express the lateral limits of the sedimentation of the head of the flows or shear structure followed by filling resulting from re-sedimentation of the tail and body of the flows. The mixture of pedosediments with arkose quartz sediments from the sedimentation plane denotes friction and shear between the flow and the sandy bed, prevalent in turbulent flows. The flow turbulence was sufficient to generate an erosional depression at the beginning of the sedimentation plane, a phenomenon only detected in the R14 deposit (Cv 8.76%). Thin sections transverse to deposits R13 and R14 revealed a sequence of ridges and cavities characteristic of flow deposits with low (Cv ~ 3%) relative volumetric concentration of pedosediments, interpreted as surface structures of the parting lineations type.

The sediment mixture and the erosional depression-like bed morphology were also generated by flows with low volumetric concentrations (Cv ~ 3%) of pedosediments. The internal organization of moderate to poorly selected, as well as the massive to inverse fabric, was also found in deposits of flows of low (Cv ~ 3%) and transitional to high (Cv > 14%) relative volumetric concentration of pedosediments. On the other hand, in deposits with low volumetric concentrations of pedosediments (Cv ~ 3%), the massive and inverse fabric occurs associated with diffuse microlaminations of the crossed and folded type. At the same time, the inclined inverse fabric of flow R14 was also detected in transitional deposits of high (> 14%) relative volumetric concentration of pedosediments. The escape of fluids (air and water) is common to deposits R13 (Cv 6.19%) and R14 (Cv 8.76%), as well as deposits from flows with low (~ 3%) and transitional to high (> 14%) relative volumetric concentrations of pedosediments. The escape of fluids in the laminations suggests that fluidization was one of the support mechanisms for pedosediments during deposition (LOWE, 1976). However, the occurrence of dispersive pressures between grains may be the predominant mechanism (LOWE, 1982). Finally, it is worth highlighting that there are different circumstances responsible for the development of the massive fabric, from en masse deposition to deposition by gradual aggradation (WALKER, 1978; LOWE, 1982; KNELLER; BRANEY, 1995), while the inverse fabric denotes a certain degree of sediment concentration, promoting a kinematic sieving effect during sedimentation (SOHN, 1997).

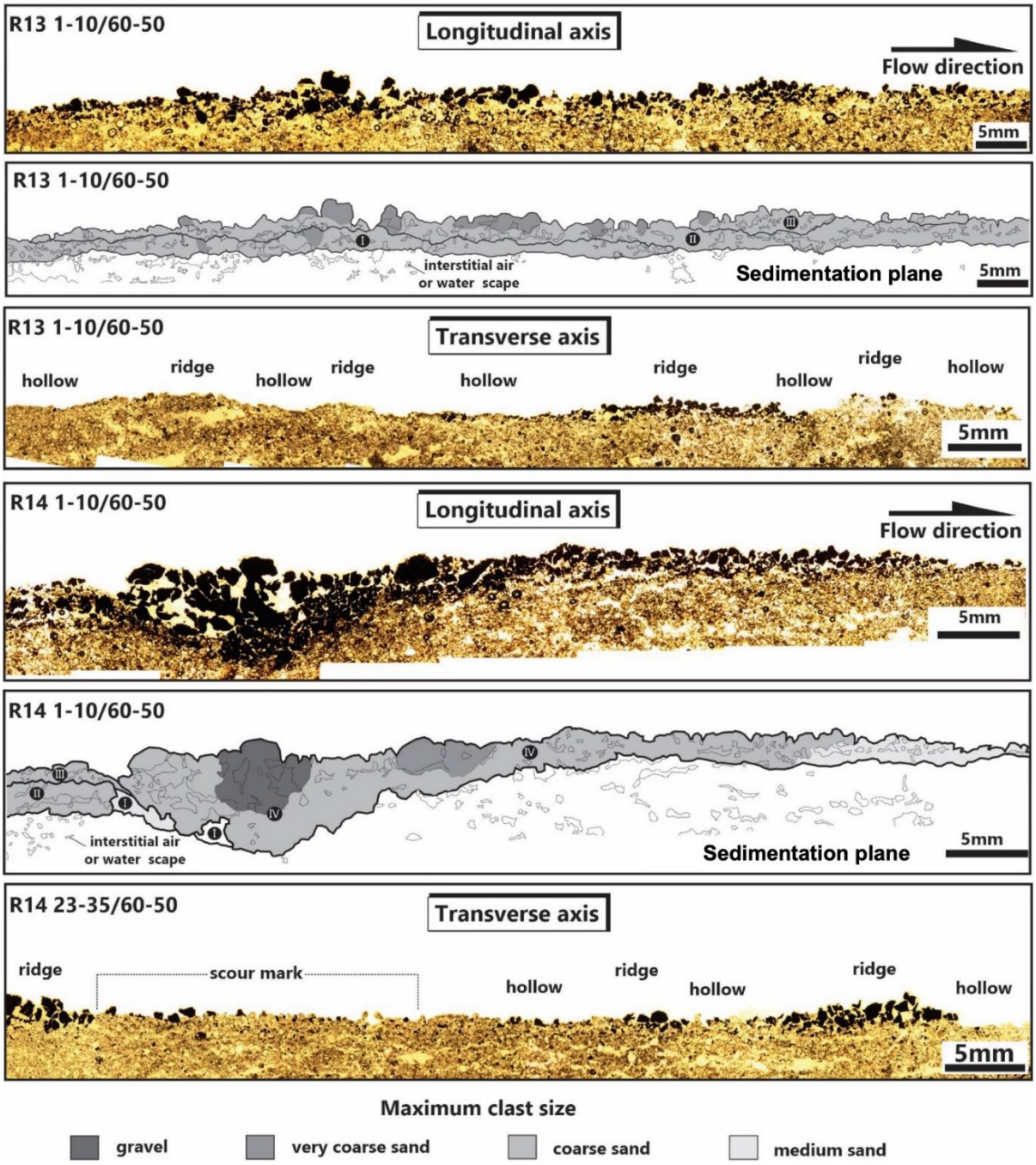

Figure 5 – Images and diagrams displaying the microstratigraphy of flow deposits R13 on R14 on the sedimentation plane.
Source: Authors (2023).

Table 1 – Microstratigraphic description of flow deposits R13 and R14 – Thin sections.

		External organization	**Internal organization**		
Lc[1]	**At[2] (mm)**	**Upper Limit[3]**	**Texture[4], composition, sphericity-rounding[5]**	**Selection[6]**	**Fabric**
R13					
1-10/60-50					
III	1.58	Continuous, wavy, non-parallel	Sand, mixture of pedossediments and arcosian quartz, very angular to sub-rounded, low to high sphericity	Poorly selected	Massive to inverse gradation, interstitial fluid (air or water)
II	1.65	Continuous, wavy, non-parallel	Sand, mixture of pedossediments and arkose quartz, very angular to sub-rounded, low to high sphericity	Poorly selected	Massive to inverse gradation, interstitial fluid (air or water)
I	1.63	Discontinuous, wavy, non-parallel	Sand, mixture of pedossediments and arkose quartz, very angular to sub-rounded, low to high sphericity	Poorly selected	Massive to inverse gradation, interstitial fluid (air or water)
Scour marks sector - 12-23/60-50					
II	5.83	Discontinuous, wavy, non-parallel	Gravelly sand, mixture of pedossediments and arkose quartz, very angular to sub-rounded, low to high sphericity	Poorly selected	Massive to inverse gradation, interstitial fluid (air or water)
I	3.55	Discontinuous, wavy, non-parallel	Gravelly sand, mixture of pedossediments and arkose quartz, very angular to sub-rounded, low to high sphericity	Poorly selected	Massive
R14					
1-10/60-50					
IV	4.20	Continuous, wavy, non-parallel	Gravelly sand, mixture of pedossediments and arkose quartz, very angular to sub-rounded, low to high sphericity	Poorly selected	Cut-and-fill with massive to inverse gradation and laterally inclined, insterstitial fluid (air or water)
III	1.00	Continuous, wavy, non-parallel	Sand, mixture of pedossediments and arkose quartz, very angular to sub-rounded, low to high sphericity	Poorly selected	Massive to inverse gradation and laterally inclined, insterstitial fluid (air or water)
II	2.00	Discontinuous, wavy, non-parallel	Sand, mixture of pedossediments and arkose quartz, very angular to sub-rounded, low to high sphericity	Poorly selected	Massive to inverse gradation, interstitial fluid (air or water)

I	0.70	Discontinuous, wavy, non-parallel	Sand, mixture of pedossediments and arkose quartz, very angular to sub-rounded, low to high sphericity	Moderately selected	Massive to inverse gradation, interstitial fluid (air or water)
Scour marks sector - 23-35/60-50					
III	1.50	Discontinuous, wavy, non-parallel	Gravelly sand, mixture of pedossediments and arkose quartz, very angular to sub-rounded, low to high sphericity	Poorly selected	Massive
II	1.30	Discontinuous, wavy, non-parallel	Sand, mixture of pedossediments and arkose quartz, very angular to sub-rounded, low to high sphericity	Poorly selected	Massive
I	1.15	Discontinuous, wavy, non-parallel	Sand, mixture of pedossediments and arkose quartz, very angular to sub-rounded, low to high sphericity	Moderately selected	Massive

[1]Lc: Lamination code
[2]At: Average thickness
Based on [3]Campbell (1967), [5]Powers (1953), [6]Harrel (1983).
[4]Ternary diagram for conglomerates (NICHOLS, 1999).

Source: Authors (2023).

4. Final considerations

The present study sought to understand the effects of sediment concentration on the generation of surface and bed sedimentary structures resulting from overland flow. The questions that guided the research were developed based on the results of previous physical experiments in the laboratory. Hence, the critical question to be answered was: do simulations of surface flow with pedosediment concentrations from 6 to 8% generate deposits similar to lower (Cv ~ 3 %) or higher (Cv 14-25 %) relative concentrations? Two experiment replications (R13 and R14) exhibited concentrations in these ranges, and their average velocities, Froude and Reynolds numbers, and the resulting deposits were analyzed. Anomalies in the decreasing trend in Froude number values during sedimentation and the presence of scour marks may represent the action of a thrust wave of the flow's tail and body in response to the deceleration of the flow's head. Vertical accretion-type surface structures, elongated arrangement, and marginal dykes are common to deposits resulting from flows R13 and R14 and flows with Cv >14% (transitional to high density). The more pronounced scour marks, partition lineations, and bed structure with a mixture of pedosediments with arkose quartz from the sedimentation plane is common to the deposits of both flows. These structures are found in flow deposits of relatively lower (Cv ~ 3%) concentration (low density). The texture of the laminations resulting in the deposits of these flows is similar in terms of external and internal organization, with subtle differences. Thus, overland flows with pedosediment concentrations of 6 to 8% generate deposits similar to flows of both lower (Cv ~ 3%) and higher (Cv 14-25%) relative concentrations, representing a continuum between low-density flows and transitional flows between low and high densities. The results suggest that, as recommended in the literature for other sedimentary environments, in the case of overland flow, it is not possible to establish an absolute value of sediment concentration or pedosediments in the context of this study to delimit low-density flows from high-density or transitional to high-density flows. These findings are essential to discerning the general dynamics of surface flow for

pedosediment deposits. However, further work is required to understand the characteristics of the flows responsible for reworking ancient colluvium into pediment ramps in northeast Brazil.

Aknowledgements

To CNPq (Proc. 302976/2021-3) and the Araucaria Foundation of Paraná (Agreement n. 072/2021 e 288/2022) for funding the research.

References

Abrahams, A. D.; Parsons, A. J.; Luk, S. H. Resistance to overland flow on desert hillslopes. *Journal of Hydrology*, n.88, 343–363, 1986.

Alberts, E. E.; Moldenhauer, W. C.; Foster, G. R. Soil aggregates and primary particles transported in rill and interrill flow. *Soil Science Society of America Journal*, n. 44, 590–595, 1980.

Ali, M.; Sterk, G; Seeger, M.; Boersema, M. P.; Peters, P. Effect of hydraulic parameters on sediment transport capacity in overland flow over erodible beds. *Hydrology and Earth System Sciences*, n. 16, 591-601, 2011.

Bennet, S.J.; Ashmore, P.; Neuman, C. M. Transformative geomorphic research using laboratory experimentation. *Geomorphology*, n. 244, 1-8, 2015.

BENVENUTI, M.; MARTINI, I. P. Analysis of terrestrial hyperconcentrated flows and their deposits. In: Martini, V. R.; Baker, V. R.; Garzón, G. (Eds.). *Flood and megaflood processes and deposits: recent and ancient examples.* Spec. Publ. Int. Ass. Sediment. n.32, 2002. p.167-193.

BERTRAN, P., FRANCOU, B. AND TEXIER, J. P. Stratified slope deposits: the stone-banked sheets and lobes model. In: Slaymaker, O. (Ed.). *Steepland geomorphology*. John Wiley and Sons: New York, 1995, p.147-169.

Blikra, L. H.; Nemec, W. Posglacial colluvium in western Norway: depositional processes, facies and palaeoclimatic record. *Sedimentology*, n. 45, 909-959, 1998.

Campbell, C. V. Lamina, laminaset, bed and bedset. *Sedimentology*, n. 8, 7-36, 1967.

Cartigny M. J. B.; Ventra, D.; Postma, G.; Van der Berg, J.H. Morphodynamics and sedimentar structures of bedforms under supercritical-flow conditions: new insights from flume experiments. *Sedimentology*, n. 61: 712-748, 2014.

CORRÊA, A.C.B.; MONTEIRO, K.A. Geomorphological dynamics of the elevated geosystems of the Borborema Highlands, Northeast of Brazil, from optically stimulated luminescence dating of hillslope sediments. *William Morris Davis - Revista de Geomorfologia*, v. 1, n. 1, 2020, p. 162-185.

Dasgupta, P. Sediment gravity flow – the conceptual problems. *Earth-Science Reviews*, n. 62, 265-281, 2003.

FITZPATRICK, E. A. *The micromorphology of soils: a manual for the preparation and description of thin sections of soils*. Aberdeen, Soil Science, 1980, 380 p.

Fonseca, D. N; Silva, A. C. da; Barros, A. C. M. de; Silva, J. C. B. da; Silva, O. G. da. Mapeamento morfodinâmico como suporte à análise de processos de degradação em áreas do município de Cabrobó – Pernambuco. *Revista da Casa da Geografia de Sobral*, v. 19, n. 2, p. 92-107, 2017.

Guo, Z.; Ma, M.; Cai, C.; Wu, Y. Combined effects of simulated rainfall and overland flow on sediment and solute transport in hillslope erosion. *Journal of Soils and Sediments*, n. 4, 1-13, 2017.

Harrell, J. A visual comparator for degree of sorting in thin and plane sections. *Journal of Sedimentary Research*, n. 54, 646-650, 1983.

Kneller, B. C.; Branney, M. J. Sustained high-density turbidity currents and the deposition of thick massive sands. *Sedimentology*, n. 42, 607-616, 1995.

Liu, C.; Li, Z.; Fu, S.; Ding, L.; Wu, G. Influence of soil aggregate characteristics on the sediment transport capacity of overland flow. *Geoderma*, n. 369, 114338, 2020.

Lowe, D. R. Sedimet gravity flows: II. Depositional models with special, reference to the deposits of high-density turbidity currents. *Journal of Sedimentary Research*, n. 52, 279-297, 1982.

Lowe, D. R. Subaqueous liquefied and fluidized sediment flows and their deposits. *Sedimentology*, n.23, 285-308, 1976.

MANICA, R. Sediment gravity flow: study based on experimental simulations. In: Schulz, H.; Lobosco, R.; Simoes, A. (Eds.) *Hydrodynamics: natural water bodies.*), London: Interch Open, 2012, p.263-286.

Miller, B. A.; Juilleret, J. The colluvium and alluvium problem: Historical review and current state of definitions. *Earth-Science Reviews*, n. 209, 103316, 2020.

Nemec, W.; Kazanci, N**.** Quaternary colluvium in west-central Anatolia: sedimentary facies and palaeoclimatic significance. *Sedimentology*, n. 46, 139-170, 1999.

NICHOLS, G. *Sedimentology and stratigraphy*, Blackwell Science, 1999. 355 p.

Oliveira, M. A. T.; Behling, H.; Pessenda, L. C. R. Late-Pleistocene and mid-Holocene environmental changes in highland valley head areas of Santa Catarina state, Southern Brazil. *Journal of South America Earth Sciences*, n. 26, 55–67, 2008.

Oliveira, M. A. T.; Camargo, G., Paisani, J. C.; Camargo Filho, M. Caracterização paleohidrológica de estruturas sedimentares quaternárias através de análise macroscópicas e microscópicas: do registro sedimentar local aos indícios de mudanças globais. *Pesquisas em Geociências*, v. 28, n. 2, 183-195, 2001.

Paisani, J. C.; Manica, R.; Santos, M. C. P.; Ribeiro, R. A. R. Modern soil aggregate-colluvium generated by overland flow – stratigraphy and physical experiments. *Sedimentology*, online version, 1-25, 2023a.

Paisani, J. C.; Pereira, J. S.; de Sordi, M. V.; Manica, R. Pleistocene-Holocene colluvial facies from the Volcanic Plateau of the Paraná Sedimentary Basin (Rio Grande do Sul, Brazil) – sedimentation processes and paleoenvironmental implications. *Journal South American Earth Sciences*, n. 126, 104344, 2023b.

Paisani, J. C.; Santos, M. C.; de Sordi, M. V. Low-concentrated overland flow generated in laboratory experiments: sedimentar structures and fabric. *Revista Brasileira de Geomorfologia*, in press.

Paola, C.; Straub, K.; Mohrig, D.; Reinhardt, L. The "unreasonable effectiveness" of stratigraphic and geomorphic experiments. *Earth-Science Reviews*, n. 97, 1–43, 2009.

Pierson, T. C.; Costa, J. E. A rheologic classification of subaerial sediment-water flows. *Geological Society of America Reviews in Engineering Geology*, VII, 1-12, 1987.

Powers, M. C. A new roundness scale for sedimentary particles. *Journal of Sedimentary Research*, n. 23, 117-119, 1953.

Shanmugam, G. High-density turbidity currents: are they sandy debris flow? *Journal of Sedimentary Research*, n. 66, 2-10, 1996.

Sohn, Y. K. On traction-carpet sedimentation. *Journal of Sedimentary Research.*, n. 67, 502-509, 1997.

Strahler, A. Hypsometric (area-altitude) analysis of erosional topography. *Geological Society of America Bulletin*, n. 63, 1117-1142, 1952.

Ventra, D.; Dìaz, G. C.; de Boer, P. Colluvial sedimentation in a hyperarid setting (Atacama desert, northern Chile): geomorphic controls and stratigraphic facies variability. *Sedimentology*, n. 60, 1257-1290, 2013.

Walker, R. G. Deep-water sandstone facies and ancient submarine fans: models for exploration for stratigraphic traps. *American Association of Petroleum. Geologists Bulletan,* n. 62, 932-966, 1978.

Wentworth, C. K. A scale of grade and class terms for clastic sediments. *Journal of Geology*, n. 30, 377-392, 1922.